Neoplasia • Vol. 8, No. 4, April 2006, pp. 279–289 279

www.neoplasia.com

Aberrant Wnt/β-Catenin Signaling in Pancreatic Adenocarcinoma[1]

Gang Zeng[*,2], *Matt Germinaro*[*,2], *Amanda Micsenyi*[*], *Navjot K. Monga*[*], *Aaron Bell*[*], *Ajit Sood*[†], *Vanita Malhotra*[‡], *Neena Sood*[‡], *Vandana Midda*[†], *Dulabh K. Monga*[§], *Demetrius M. Kokkinakis*[*,¶] and *Satdarshan P. S. Monga*[*,¶,#]

[*]Department of Pathology, School of Medicine, University of Pittsburgh, Pittsburgh, PA, USA; [†]Department of Medicine, Dayanand Medical College and Hospital, Ludhiana, Punjab, India; [‡]Department of Pathology, Dayanand Medical College and Hospital, Ludhiana, Punjab, India; [§]Department of Human Oncology, Allegheny General Hospital, Pittsburgh, PA, USA; [¶]Cancer Institute, School of Medicine, University of Pittsburgh, Pittsburgh, PA, USA; [#]Department of Medicine, School of Medicine, University of Pittsburgh, Pittsburgh, PA, USA

This manuscript is dedicated to Satwant Kaur Monga, MD, who succumbed to pancreatic adenocarcinoma on February 10, 2001, at the age of 57 years.

Abstract

Wnt/β-catenin signaling plays an important role in normal development. However, its aberrant activation is associated with several cancers. The aim of this study is to examine the Wnt/β-catenin pathway in patients with advanced pancreatic adenocarcinoma (*n* = 31). Paraffin sections from tumors (*n* = 16) and normal pancreata (*n* = 3) were used to determine the localization of β-catenin. An additional 15 frozen tumors, adjacent normal pancreata (*n* = 5), or normal pancreata (*n* = 4) were utilized for protein isolation. Tumors were also examined for mutations in exon 3 of the *CTNNB1* gene. More than 65% of the tumors showed an increase in total β-catenin, consistent with its enhanced membranous, cytoplasmic, and nuclear localization, but only two showed mutations in *CTNNB1*. The majority of the remaining tumors demonstrated concurrent increases in Wnt-1 and frizzled-2 (positive regulators) and a decrease in Ser45/Thr41-phospho-β-catenin. Electrophoretic mobility shift assay demonstrated β-catenin–T-cell factor binding in tumors only. Adenomatous polyposis coli and axin, which are both negative regulators, remained unchanged. Unexpectedly, total glycogen synthase kinase-3β protein was elevated in these tumors. Elevated levels of E-cadherin were also observed, although E-cadherin–β-catenin association in tumors remained unaffected. Thus, Wnt/β-catenin activation was observed in 65% of pancreatic adenocarcinomas, independently of β-*catenin* gene mutations in most tumors.

Neoplasia (2006) **8,** 279–289

Keywords: Pancreas, tumors, mutation, patient, cancer.

Background

Pancreatic adenocarcinoma is among the most devastating cancers. It is responsible for 5% to 6% of all cancer-related deaths and has recently replaced prostate as the fourth major cause of cancer-related mortality in the United States [1]. It remains a disease of poor prognosis with a 5-year survival rate of <4%, which has remained unchanged in the last four decades [2]. The poor prognosis of pancreatic cancer mandates the exploration of potential mechanisms that might contribute to the pathogenesis of this disease and its resistance to therapy.

The Wnt/β-catenin pathway has been implicated in tumorigenesis at several sites, including the colon, rectum, lung, skin, breast, and liver [3–7]. Aberrant signaling involving stabilization of β-catenin, along with its nuclear translocation, and activation of target genes such as *c-myc* and *cyclin D1* have been observed in these cancers [8,9]. This pathway has also been shown to be involved in normal development and tissue regeneration [10,11].

Recent studies have also established a developmental relationship between the pancreas and the liver [12]. There appears to be a common stem cell that forms a ventral pancreas or a primitive liver on appropriate signaling. This suggests that some molecular signals may be shared by the liver and the pancreas during development and, thus, also in cancer. A significant number of hepatoblastomas and hepatocellular cancers have demonstrated aberrant β-catenin accumulation and signaling [13]. Some pediatric pancreatic tumors, such as pancreatoblastomas, have also shown such abnormal reactivity [14,15]. Although there have been some analyses of this pathway in pancreatic adenocarcinoma through immunohistochemistry, reports have been conflicting [16,17].

The Wnt/β-catenin pathway is regulated transcriptionally and posttranscriptionally. Its central component, β-catenin, is phosphorylated in the inactive phase of this pathway in the

Address all correspondence to: Satdarshan P. S. Monga, MD, School of Medicine, University of Pittsburgh, 200 Lothrop Street, S421-BST, Pittsburgh, PA 15261. E-mail: smonga@pitt.edu

[1]This work was funded, in part, by the Rangos Fund for Enhancement of Pathology Research, ACS (grant RSG-03-141-01-CNE to S.P.S.M.), and the National Institutes of Health (grant 1RO1DK62277 to S.P.S.M.)

[2]Gang Zeng and Matt Germinaro contributed equally to this work.

DOI 10.1593/neo.05607

absence of Wnt or in the presence of Wnt inhibitors [18,19]. This results in the phosphorylation of β-catenin by glycogen synthase kinase-3β (GSK3β) or casein kinases. With the aide of adenomatous polyposis coli (APC) gene product and axin, it is presented to β-transducin repeat-containing protein for proteosomal degradation. In the presence of Wnt or frizzled upregulation, or due to mutations affecting exon 3 of the β-*catenin* gene (*CTNNB1*) that impact the Ser/Thr sites of β-catenin, or APC or axin, β-catenin protein becomes stable and translocates to the nucleus to turn on target gene expression. In the present study, we investigate the status of Wnt/β-catenin pathway and identify this novel molecular aberration and its mechanism in pancreatic adenocarcinoma patients.

Methods

Patient Tissue

All tissues and materials used in this study were obtained under an approved Institutional Review Board (exempt) protocol. Paraffin sections from the pancreatic adenocarcinoma of 16 patients (T1–T16) and three normal pancreatic sections (N1–N3) were obtained from the Department of Pathology, School of Medicine, University of Pittsburgh (Pittsburgh, PA; *n* = 10) and the Department of Pathology and Gastroenterology, Dayanand Medical College and Hospital (Ludhiana, Punjab, India; *n* = 6). Relevant patient information and tumor histology are presented in Table 1. Frozen tissues from 15 additional patients, along with adjacent normal pancreata in five cases and four independent normal autopsy specimens of pancreata, were obtained from the Department of Pathology Tissue Bank, School of Medicine, University of Pittsburgh, and the Cooperative Human Tissue Network, Eastern Division (Philadelphia, PA). Pertinent patient and tumor information, along with examined controls, is detailed in Table 2 (FT1–FT15). The tumor–node–metastasis (TNM) status of three tumors was not available, and one tumor was classified as $T_4N_0M_x$ due to recurrence in the pancreas and soft tissue involvement.

Histology and Immunohistochemistry

Paraffin sections from tumors (*n* = 16) and normal human pancreata (*n* = 3) were used for immunohistochemical staining. Sections were passed through a sequence of xylene and graded alcohol and then rinsed in phosphate-buffered saline (PBS). Endogenous peroxidase was inactivated using 3% hydrogen peroxide (Sigma, St. Louis, MO). Sections were placed in blue blocker (Shandon Lipshaw, Pittsburgh, PA) then incubated for 2 hours at room temperature with a primary antibody (diluted to 2.5–5 μg/ml in PBS) that also contains 1 mg/ml bovine serum albumin (BSA). Slides were placed in the microwave on high power twice for 10 minutes in citrate buffer. For each successive step, four 5-minute rinses in PBS were performed. The sections were incubated in PBS containing an appropriate secondary antibody (Chemicon, Temecula, CA) for 1 hour at room temperature. The signal was detected using the ABC Elite kit (Vector Laboratories, Burlingame, CA), as prescribed in the manufacturer's instructions. Color development was closely monitored under a microscope. Sections were counterstained with modified Harris hematoxylin solution (Sigma). Following dehydration, by passage through graded alcohol concentrations and xylene, sections were coverslipped and mounted using DPX (Fluka Laboratories, St. Louis, MO). For negative control, the sections were incubated with secondary antibodies only. Slides were viewed on an Axioskop 40 (Zeiss, Thornwood, NY) upright research microscope, and digital images were obtained by a Nikon Coolpix camera (Nikon, Melville, NY). Collages were prepared using Adobe Photoshop software (Adobe, San Jose, CA).

Genomic DNA Preparation and Mutational Analysis

Genomic DNA was extracted using DNAzol reagent (Molecular Research Center, Inc., Cincinnati, OH). The DNA was dissolved in 20 μl of 10 mM Tris–HCl (pH 8.0). To amplify the

Table 1. Patient Data (for Immunohistochemistry Analysis).

Patient Number	Age Range (years)	Sex	Tumor Histology	TNM Classification	Anatomic Location
T1	60–69	M	Moderately differentiated adenocarcinoma, invasive	$T_3N_1M_x$	Entire length
T2	40–49	M	Moderately differentiated adenocarcinoma, invasive	$T_3N_1M_x$	Head
T3	70–79	M	Moderately differentiated adenocarcinoma, invasive	$T_3N_0M_x$	Distal/tail
T4	60–69	M	Moderately differentiated adenocarcinoma, invasive	$T_3N_1M_x$	Head
T5	70–79	F	Moderately differentiated adenocarcinoma, invasive	$T_3N_1M_x$	Head
T6	80–89	M	Moderately differentiated adenocarcinoma, invasive	$T_3N_1M_x$	Distal/tail
T7	50–59	F	Poorly differentiated adenocarcinoma, invasive	$T_3N_1M_x$	Head
T8	70–79	F	Poorly differentiated adenocarcinoma, invasive	$T_3N_1M_x$	Head
T9	70–79	F	Moderately differentiated adenocarcinoma, infiltrative	$T_2N_0M_x$	Ampulla of Vater
T10	70–79	M	Poorly differentiated adenocarcinoma, invasive	$T_3N_0M_x$	Head
T11	50–59	M	Moderately differentiated adenocarcinoma	NA	Head
T12	40–49	F	Moderately differentiated adenocarcinoma	NA	Body
T13	40–49	M	Moderately differentiated adenocarcinoma, invasive	NA	Head
T14	60–69	M	Moderately differentiated adenocarcinoma	NA	Head
T15	40–49	F	Moderately differentiated adenocarcinoma	NA	Head
T16	40–49	F	Moderately differentiated adenocarcinoma	NA	Head

M, Male; *F*, female.

Table 2. Patient Data (for Frozen Tissue Analysis).

Number	Age Range (years)	Sex	Histology	TNM	Tumor Location	Control (Label)
FT1	70–79	F	Moderately differentiated adenocarcinoma, invasive	$T_3N_1M_x$	Head	Adjacent normal pancreas (FN1)
FT2	50–59	M	Poorly differentiated adenocarcinoma, invasive	$T_3N_1M_x$	Distal/tail	Adjacent normal pancreas (FN2)
FT3	80–89	M	Moderately differentiated adenocarcinoma, invasive	$T_4N_0M_x$	Distal/tail	Adjacent normal pancreas (FN3)
FT4	70–79	F	Moderately to poorly differentiated adenocarcinoma, invasive	$T_2N_0M_x$	Head	Adjacent normal pancreas (FN4)
FT5	70–79	F	Moderately to poorly differentiated adenocarcinoma, invasive	$T_3N_1M_1$	Uncinate process/head	Adjacent normal pancreas (FN5)
FT6	50–59	M	Moderately differentiated adenocarcinoma, invasive	Unavailable	Head	No adjacent available (N1–N4)
FT7	70–79	M	Moderately differentiated adenocarcinoma, invasive	Unavailable	Head	Adjacent normal stomach (N7)
FT8	70–79	F	Poorly differentiated adenocarcinoma, invasive	Unavailable	Distal/tail	Adjacent normal spleen (N8)
FT9	60–69	F	Moderately differentiated adenocarcinoma	$T_2N_1M_x$	Head	No adjacent available (N1–N4)
FT10	60–69	F	Moderately differentiated adenocarcinoma	$T_3N_0M_x$	Head (distalmost margin)	No adjacent available (N1–N4)
FT11	60–69	M	Moderately differentiated adenocarcinoma, invasive	$T_3N_1M_x$	Distal/tail	No adjacent available (N1–N4)
FT12	50–59	M	Moderately to poorly differentiated adenocarcinoma	$T_3N_0M_x$	Distal/hilum	No adjacent available (N1–N4)
FT13	60–69	F	Moderately differentiated adenocarcinoma	$T_2N_0M_x$	Tail	No adjacent available (N1–N4)
FT14	50–59	F	Moderately differentiated adenocarcinoma	$T_4N_0M_x$	Head	No adjacent available (N1–N4)
FT15	60–69	M	Poorly differentiated adenocarcinoma	$T_1N_0M_x$	Distal	No adjacent available (N1–N4)

Number	Age (years)	Sex	Cause of Death	Histology (Pancreas)	Medical History
N1	40–49	M	Acute renal failure	Normal	Not significant, nonsmoker, social drinker
N2	70–79	M	Acute myocardial infarction	Normal	Not significant, proton pump inhibitors, nonsmoker, nonalcoholic
N3	80–89	F	Atherosclerotic vascular disease	Normal	Memory loss, no other significant history, no significant history of smoking/alcohol intake
N4	80–89	F	Not determined/dementia	Normal	Dementia, memory loss, nonsmoker/nonalcoholic

M, Male; *F*, female; *FT*, frozen pancreatic tumors; *FN*, frozen adjacent normal pancreas; *N1–N4*, true normal pancreata from autopsies.

exon 3 of the human β-catenin (*CTNNB1*) gene, polymerase chain reaction (PCR) was performed using hCat-E3-S2 sense primer (5′-CCCTGGCTATCATCTGCTTT-3′) and hCat-E3-AS2 antisense primer (5′-CACTCACTATCCACAGTTCAGCA-3′). The amplified product of 545 bp also included a 230-bp fragment of *CTNNB1*'s exon 3. The thermal cycler was programmed as follows: initial denaturation at 94°C for 2 minutes and 35 amplification cycles for the first PCR; one amplification cycle comprising denaturation at 94°C for 30 seconds, annealing at 58°C for 30 seconds, and extension at 72°C for 1 minute; and the final extension at 72°C for 10 minutes. PCR products were confirmed by agarose gel electrophoresis, purified using QIAquick Gel Extraction Kit (Qiagen, Valencia, CA), and submitted to direct sequencing using the ABI Big Dye Terminator Cycle Sequencing kit (Applied Biosystems, Foster City, CA) and the primers used for PCR.

Whole Cell Lysate Preparation

Frozen tumors ($n = 15$) and all normal controls (in Table 2) were utilized for total cell lysate preparation. Homogenization tubes were initially filled with 200 μl of RIPA buffer (9.1 mM dibasic sodium phosphate, 1.7 mM monobasic sodium phosphate, 150 mM sodium chloride, 1% Nonidet P-40, 0.5% sodium deoxycholate, and 0.1% sodium dodecyl sulfate, pH adjusted to 7.4). A fresh protease and phosphatase inhibitor cocktail was also added (Sigma). To determine the protein concentration of the lysates, a bicinchoninic acid protein assay was performed, with BSA as standard.

Gel Electrophoresis and Western Blot Analysis

All data shown are representative of three determinations. Ready gels (7.5%, in 50-μl wells) were loaded with 100 μg of protein from prepared cell lysates using the mini-PROTEIN 3 electrophoresis module assembly (Bio-Rad, Hercules, CA). Protein was transferred overnight (0.09 A, 4°C) to Immobilon-PVDF membranes (Millipore, Bedford, MA) with the Mini Trans-Blot Electrophoretic Transfer Cell (Bio-Rad) in transfer buffer (25 mM Tris pH 8.3, 192 mM glycine, 20% methanol, and 0.025% sodium dodedyl sulfate). Depending on the antibody, blots were then blocked for 1 hour in either 5% nonfat dry instant milk or 5% BSA, both in Tris-buffered saline–Tween. Next, blots were incubated with primary antibody for 3 hours at room temperature or overnight at 4°C. Following incubation, blots were washed for 5 minutes (×3) in 1% milk blotto/1% BSA. One-hour incubation with horseradish peroxidase (HRP)–conjugated secondary antibody in 1% milk blotto/1% BSA took place after the washes. Another series of washes was administered (3 × 5 minutes) before blots were subjected to fresh Super-Signal West Pico Chemiluminescent Substrate (Pierce, Rockford, IL) for exactly 5 minutes. The

blots were then visualized by autoradiography. Once scanned, densitometric analysis was employed on the autoradiographs by means of an NIH Imager software (Bethesda, MD). IgG elution buffer (Pierce) was used at room temperature (two 30-minute washes) to strip the blots for reprobing.

Primary antibodies utilized in this study were against β-catenin, E-cadherin, frizzled-1/2, GSK3β, APC, axin, *cyclin D1*, and *c-myc* (Santa Cruz Biotechnology, Santa Cruz, CA); Wnt-1 (Upstate Biotechnology, Lake Placid, NY); Ser45/Thr41–β-catenin and Ser33,37/Thr41–β-catenin (Cell Signaling, Beverly, MA); and actin (Chemicon). HRP-conjugated secondary antibodies (Chemicon) were utilized at 1:50,000 or 1:75,000 dilutions.

Immunoprecipitation

Five hundred micrograms of protein lysate from tumor and normal samples was brought to a volume of 1 ml using RIPA buffer and precleared by employing appropriate control IgG along with 20 μl of Protein A/G agarose (Santa Cruz Biotechnology). Following overnight end-over-end rotation in a cold room (4°C), the samples were centrifuged to form a pellet. The obtained supernatant was then transferred to a new set of 1.5-ml tubes. Twenty microliters of agarose-conjugated goat anti–β-catenin antibody (Santa Cruz Biotechnology) was added, and the tubes were incubated overnight (4°C). Subsequently, pellets were collected by centrifugation and subjected to a series of RIPA washes at 4°C followed by centrifugation. The pellets were then resuspended in equal volumes of standard electrophoresis loading buffer with sodium dodecyl sulfate and fresh β-mercaptoethanol and boiled for 5 minutes. Lastly, the samples (30 μl each) were resolved on ready gels and transferred as described in Gel Electrophoresis and Western Blot Analysis.

Nuclear Protein Isolation and Electrophoretic Mobility Shift Assay (EMSA) for β-Catenin Activation

Frozen tissues (0.2–0.5 g) from 10 tumors that showed increases in total β-catenin protein and their respective controls were finely sliced and homogenized in a glass Dounce homogenizer (50–100 strokes) in 1 ml of hypotonic buffer [10 mM HEPES pH 7.9, 10 mM NaH_2PO_4, 1.5 mM $MgCl_2$, 1 mM DTT, 0.5 mM Spermidine, and 1 M NaF, with protease and phosphatase inhibitor cocktails (P8340, P5726, and P2850; Sigma) used at 1/100 dilution]. Homogenization was monitored under a microscope using Trypan blue to control for the release of nuclei. Homogenates were centrifuged for 5 minutes at 800*g*. Nuclei pellets were washed, repelleted twice in 2 ml of hypotonic buffer, and snap-frozen in liquid nitrogen.

Nuclear proteins were extracted in 25 to 50 μl of hypertonic buffer [30 mM HEPES pH 7.9, 25% glycerol, 450 mM NaCl, 12 mM $MgCl_2$, 1 mM DTT, and 0.1 mM EDTA, with protease and phosphatase inhibitor cocktails (P8340, P5726, and P2850; Sigma) used at 1/200 dilution] for 30 to 45 minutes at 4°C with continuous agitation. Extracts were centrifuged at 30,000*g* for 30 minutes. Supernatants were collected, and protein concentration was determined by bicinchoninic acid assay with BSA as standard.

EMSA was performed by incubating 5 μg of nuclear protein (n = 5) extracts with a ^{32}P-end–labeled oligonucleotide containing the core T-cell factor (TCF)/lymphoid enhancer factor (LEF) binding site of the *cyclin D1* promoter (5′-TGC CGG GCT TTG ATC TTT GCT-3′) at room temperature for 20 minutes. The binding reaction conditions were 15 mM HEPES pH 7.9, 75 mM NaCl, 6 mM $MgCl_2$, 0.025 mM EDTA, 2.5 mM Tris pH 7.6, 12.5% glycerol, and 1 mM DTT, with protease and phosphatase inhibitor cocktails (P8340, P5726, and P2850; Sigma) used at 1/400 dilution. Reaction products were analyzed on a 5% nondenaturing polyacrylamide gel using 0.5% Tris–borate–EDTA buffer. The specificity of the DNA-binding complex was determined by adding ×20 cold TCF/LEF oligo as competitor. Gels were dried and exposed to BioMax MR film (Eastman Kodak, Rochester, NY).

Quantitative and Statistical Assessment

Immunohistochemistry was examined by a single pathologist and scored for β-catenin staining based on intensity. The staining intensity of β-catenin at the membrane, cytoplasm, and nuclei of tumor cells (ductal cells), or of ductal cells in normal samples was scored (1–3) to calculate an arbitrary immunohistochemical score. Five individual fields (×400) from each section were examined and noted for β-catenin staining intensity and redistribution in tumor cells or ductal cells in the tumors and normal pancreata, respectively. Because of differences in the cellular composition of the tumors and the normal pancreata, quantitative assessment excluded differences in the number of positively staining cells and was chiefly based on the intensity of staining and the redistribution of β-catenin protein in a single cell type (ductal cells). Mean ± SEM scores for tumors (n = 16) and normal samples (n = 3) were averaged and compared for statistical significance by Student's t test ($P < .05$ was considered significant).

Autoradiographs were scanned and analyzed for densitometry by an NIH Imager 1.58 software. The integrated optical density (IOD) obtained from this analysis was normalized to the value obtained from normal tissues. Differences in IOD were represented as fold changes and were graphically presented using the KaliedaGraph software (Synergy Software, Reading PA).

Results

Redistribution of β-Catenin in Pancreatic Adenocarcinoma

Paraffin sections from pancreatic adenocarcinoma and normal pancreas were assessed for β-catenin localization. In the normal pancreas, β-catenin is predominantly localized at the membrane of the ductal cells in the exocrine pancreas (Figure 1*A*). In addition, it is found in the cytoplasm or nucleus in less than 1% to 3% of these cells.

An overall increase in the intensity of β-catenin staining was detected in the cytoplasm and nucleus of 11 of 16 tumors (Figure 1, *B–G*). Interestingly, the membranous localization of β-catenin in all tumor samples remained relatively intact irrespective of an increase in its cytoplasmic or nuclear

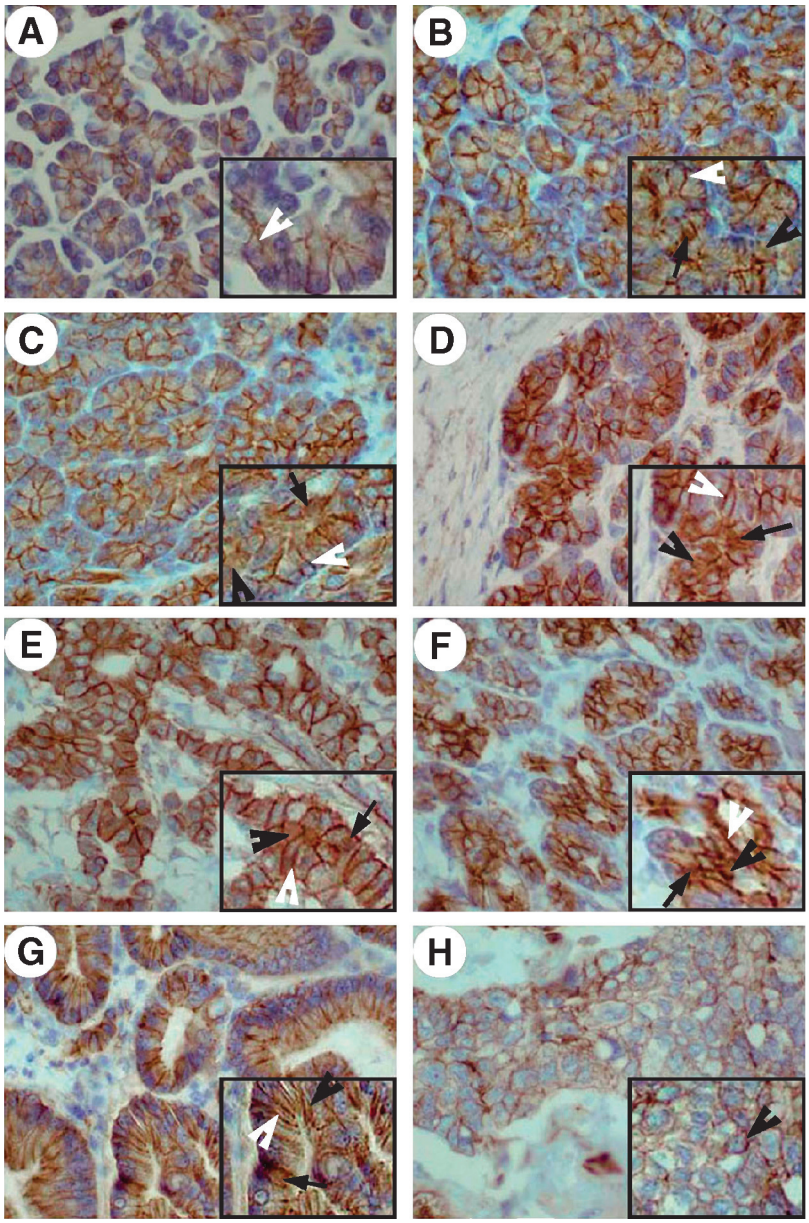

Figure 1. *β-Catenin undergoes redistribution in the majority of pancreatic adenocarcinomas. (A) A representative section from a normal pancreas, obtained through autopsy, shows predominantly membranous localization in tall columnar acinar cells. Inset: Higher magnification highlights membranous localization (white arrowhead). (B–G) Representative tumors from six patients show aberrant β-catenin localization. Insets: Higher magnification clearly demonstrates increased nuclear (arrow) and cytoplasmic (arrowhead) β-catenin localization in pancreatic adenocarcinoma, while still maintaining membranous localization (white arrowhead). (H) A representative tumor from the minor subset of tumors shows normal membranous localization of β-catenin. Inset: Higher magnification shows membranous localization (white arrowhead) of β-catenin in this tumor.*

localization. The remaining five tumors did not exhibit any change in β-catenin staining in terms of intensity or localization and were similar to the normal pancreas; one representative section is shown (Figure 1*H*). For quantitative assessment, the arbitrary immunohistochemistry score based on staining intensity at the membrane, cytoplasm, and nucleus of the ductal cells in the tumors ($n = 16$) and normal pancreata ($n = 3$) showed a statistically significant difference ($P < .05$; Figure 2). Eleven of 16 tumors displayed increased staining for β-catenin (score $\geq$ 5/9) compared to the normal samples or tumors that showed no change (score $\leq$ 2/9) (Table 3). Thus, an aberrant increase in β-catenin staining was detected in around 68% of pancreatic tumors, suggesting the activation of the Wnt/β-catenin pathway.

Increased β-Catenin Protein in Tumors

Protein lysates from frozen tumors ($n = 15$) and adjacent normal pancreata ($n = 5$) were analyzed for total β-catenin levels. Ten of 15 tumors showed increased levels of total β-catenin protein compared to adjacent or true normal controls shown in representative blots (Figure 3*A*). This increase ranged from two- to five-fold. Thus, more than 65% of examined frozen tumors demonstrated a notable increase in total β-catenin protein by Western blot analysis. The same lysates

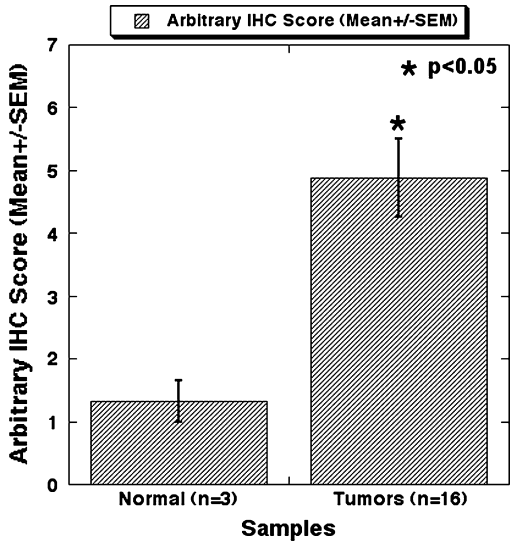

Figure 2. *An approximately five-fold increase in arbitrary immunohistochemical score was observed in pancreatic tumors (n = 16) versus normal pancreata (n = 3), which was statistically significant (P < .05).*

were used to determine levels of *c-myc* and *cyclin D1*—the known targets of the Wnt/β-catenin pathway. There was a small increase in the total c-myc protein in three of six tumors that displayed an increase in β-catenin protein, whereas the three others remained unchanged (Figure 3*B*). Surprisingly, the two remaining samples that showed no change in total β-catenin protein also showed a noteworthy increase (greater than five-fold) in total c-myc protein. A similar pattern was observed for *cyclin D1* levels also, and no direct correlation was observed in elevated β-catenin and *cyclin D1* levels (not shown). These results suggest a β-catenin–independent upregulation of *c-myc* and *cyclin D1* in pancreatic adenocarcinomas in a significant subset of such tumors.

Increased Nuclear Accumulation and DNA Binding of β-Catenin in Tumors

To verify the increased nuclear accumulation of β-catenin in tumor samples and to assess its functional relevance, we isolated nuclear protein extracts from tumors and adjacent normal tissues and analyzed them for β-catenin protein levels and DNA binding activity. All 10 samples that showed elevated total β-catenin displayed elevated nuclear β-catenin protein compared to the controls, as shown in a representative blot in Figure 3*C*. In addition, five samples were randomly selected from these 10 tumors, showing elevated total and nuclear β-catenin protein β-catenin–TCF complex formation by EMSA. The β-catenin–TCF complex was readily detected in the nuclear extracts of tumors, as shown in a representative analysis from tumor 5 and its adjacent normal pancreas (Figure 3*B*). These results demonstrate active β-catenin signaling in pancreatic adenocarcinoma.

Changes in Canonical Wnt/β-Catenin Pathway Components in Tumors

Our next aim was to examine the status of the canonical Wnt pathway in these tumors to identify additional mechanisms of β-catenin stabilization in pancreatic adenocarcinoma. To this end, we investigated the protein expression of upstream effectors of this pathway: Wnt-1 and frizzled-1/2. This was dictated by previous reports identifying these genes in normal pancreata [20,21]. Although low Wnt-1 levels were detected in normal pancreata, we wanted to examine its levels in pancreatic adenocarcinomas. Similarly, although frizzled-1 and frizzled-2 were present in normal pancreata, we were interested in identifying any changes in tumors. In addition, these components represent the canonic Wnt pathway. An increase in total Wnt-1 protein was evident in the same 8 of 10 patients who had demonstrated elevated β-catenin levels, suggesting a possible mechanism of β-catenin increase in these patients. Although the observed increase was modest, it was consistently higher in the tumors compared to controls (Figure 3). In addition, frizzled-2 demonstrated a bold increase in the same 8 of 10 tumor samples, as shown in representative Western blot analysis, whereas frizzled-1 remained undetected in tumors or controls (Figure 3). Next, we examined the tumors and normal tissue lysates for negative regulators of β-catenin, which are components of its degradation pathway. GSK3β, axin, and APC proteins were examined in pancreatic tumors and adjacent normal pancreata. All tumors showed an unexpected increase in total GSK3β levels compared to the normal or adjacent controls (Figure 3). Axin protein levels in the majority of tumors from adjacent or normal pancreata remained unchanged, whereas a minority of tumors showed increased levels of axin in tumors, which coexisted always with increased β-catenin (Figure 3). APC protein levels also displayed similar levels in tumors and adjacent normal or true normal pancreata in all cases (Figure 3). These results indicate that, although GSK3β elevation might be a compensatory or an unrelated event, the inability of axin or APC proteins to increase and thus

Table 3. Quantitative Estimation of β-Catenin Immunohistochemistry in Pancreatic Adenocarcinoma Samples.

Number	Membrane	Cytoplasm	Nucleus	Overall
T1	++	+++	++	6/9
T2	++	+++	–	5/9
T3	++	+++	+	6/9
T4	++	++	+	5/9
T5	+++	+++	–	6/9
T6	+++	+++	+	7/9
T7	+++	+++	++	8/9
T8	+	+	–	2/9
T9	+++	+++	+	7/9
T10	+	+	–	2/9
T11	++	–	–	2/9
T12	+	–	–	1/9
T13	++	++	+	5/9
T14	+++	+++	++	8/9
T15	++	+++	++	7/9
T16	+	–	–	1/9
N1	+	–	–	1/9
N2	+	–	–	1/9
N3	++	–	–	2/9

T1–T16, Paraffin sections from 16 patients; *N1–N3*, normal pancreas paraffin sections.

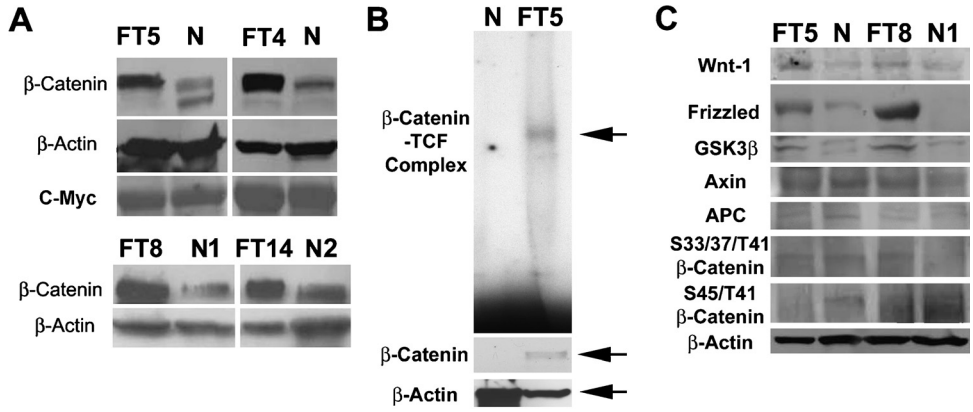

Figure 3. *Activation of the Wnt/β-catenin pathway in the majority of pancreatic adenocarcinomas. (A) Western blot analysis from four representative tumors that display increased total β-catenin protein compared to their adjacent normal pancreata (upper panel) or independent normal pancreata (lower panel). β-Actin demonstrates comparable loading of proteins. The c-myc protein remains unchanged between tumors and adjacent normal pancreata in the upper panel. (B) A representative Western blot analysis using nuclear lysates from a tumor that displayed increased total levels of β-catenin shows increased nuclear β-catenin as well. EMSA detects the β-catenin–TCF complex (arrow) in tumors and not in adjacent normal pancreas in a representative analysis. (C) Representative Western blot analyses for the status of canonical Wnt pathway in two tumors that display elevated total β-catenin reveal elevated Wnt-1 and frizzled-2 in tumors compared to normal adjacent (left set) or true normal pancreata (right set). No change in axin or APC was detected; however, an unexpected increase in GSK3β was evident in tumors only. Although Ser33,37/Thr41–phosphorylated β-catenin showed either no change (left set) or an increase in tumor (right set) compared to their respective controls, Ser45/Thr41–phosphorylated β-catenin levels were decreased in tumors, again suggesting the stabilization of β-catenin as a mechanism of its increase and activation. β-Actin blot shows equal protein loading.*

assist in β-catenin degradation may further contribute to β-catenin stabilization [22,23].

Coherent Changes in Serine–Threonine Phosphorylation of β-Catenin

To understand the functional significance of the above changes, we examined the serine–threonine phosphorylation status of β-catenin in the tumors and adjacent or true normal pancreata. Once phosphorylated at specific serine and threonine residues, β-catenin underwent degradation by ubiquitination [18]. Either Ser33,37/Thr41–phosphorylated β-catenin levels remained unaffected, or there was a modest increase in tumors, as shown in a representative blot (Figure 3). Next, we examined any differences in the levels of Ser45/Thr41–phosphorylated β-catenin, which was a more sensitive and rate-limiting step of β-catenin degradation. A consistent decrease in Ser45/Thr41–phosphorylated β-catenin was observed in 8 of 10, with elevated total β-catenin protein tumors compared to normal controls (Figure 3). This coexisted with increased levels of β-catenin, as well as Wnt-1 and frizzled, in the tumors. A small subset showed no change in Ser45/Thr41–phosphorylated β-catenin levels, despite an observed increase in β-catenin protein. This indicates an additional mechanism of β-catenin stabilization in a significant number of pancreatic adenocarcinoma (Table 4).

Mutational Analysis of Exon 3 of CTNNB1 *(β-Catenin Gene)*

Exon 3 mutations in *β-catenin* gene or *CTNNB1* have been classically associated with many tumors. Our next step was to examine the mutational status of β-catenin in the 15 frozen tumor samples. Exon 3 of *CTNNB1*, whose product contains the serine and threonine sites essential for phosphorylation and ubiquitination, was amplified by PCR. An expected size of product was obtained, ruling out any deletions as reported in other tumors [9]. The products were sequenced and examined for mutations. Two of 15 samples showed clear mutations affecting Ser33 and Ser37, respectively (Figure 4). These were single basepair alterations resulting in missense mutations. These tumors had previously shown increased levels of β-catenin protein without any changes in Wnt-1 or frizzled proteins or changes in Ser33/37/45– or Thr41-phosphorylated β-catenin levels compared to adjacent or normal pancreata (Table 4). A normal sequence was obtained from the adjacent normal pancreas of FT2 (not shown).

E-cadherin and Its Association with β-Catenin in Tumors

Another important interaction of β-catenin at the cell membrane is with E-cadherin [24,25]. A representative section

Table 4. Summary of Results of Changes in Canonical Wnt Components and *CTNNB1* Mutations in 15 Frozen Tumor Samples.

Name	Total β-Catenin Protein	Wnt-1/frizzled-2 Protein	Ser45/Thr41 β-Catenin Protein	Mutations in *CTNNB1*
FT1	NC	NC	NC	ND
FT2	I	NC	NC	S33Y (TCT→TAT)
FT3	I	I	D	ND
FT4	I	I	D	ND
FT5	I	I	D	ND
FT6	NC	NC	NC	ND
FT7	I	I	D	ND
FT8	I	I	D	ND
FT9	NC	NC	NC	ND
FT10	NC	NC	NC	ND
FT11	I	I	D	ND
FT12	I	I	D	ND
FT13	NC	NC	NC	ND
FT14	I	NC	NC	S37T (TCT→ACT)
FT15	I	I	D	ND

FT1–F15, Frozen pancreatic tumor from 15 patients; *NC*, no change; *I*, increase; *D*, decrease; *ND*, none detected.

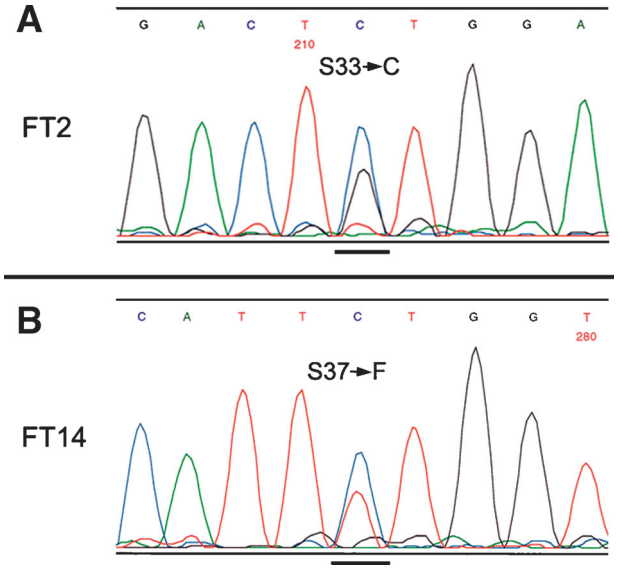

Figure 4. *Missense point mutations in the β-catenin gene in pancreatic tumors in two patients FT2 (upper panel) and FT14 (lower panel). Sequence analysis shows S33C (A) and S37F (B) mutations.*

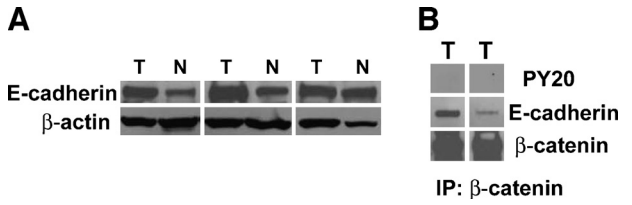

Figure 6. *Increased E-cadherin level and its continued interaction with β-catenin is observed in pancreatic adenocarcinoma. (A) Two pairs of tumors and normal pancreata at the upper left panel show increased levels of total E-cadherin in this representative Western blot analysis. The right pair shows no change. The bottom panels show β-actin as a loading control. (B) A representative coprecipitation study shows continued β-catenin–E-cadherin association (middle panel) in pancreatic adenocarcinomas in most tumors, which was a function of immunoprecipitated β-catenin in lysates (bottom panel). No tyrosine phosphorylation of β-catenin was detectable (top panel).*

from normal pancreata shows membranous distribution with minimal subcellular staining (Figure 5*A*). Analysis of the tumors revealed increased membranous and cytoplasmic localization of E-cadherin, as shown in two representative sections (Figure 5, *B* and *C*). These samples demonstrated increased β-catenin staining at the membrane as well (corresponding β-catenin staining is shown in Figure 1, *C* and *D*). Lastly, a representative section of a smaller subset of tumors is shown, which shows no change in E-cadherin localization or intensity compared to the normal pancreas (Figure 5*D*). Western blot analysis also confirmed an increase in total E-cadherin protein in the majority of tumors (Figure 6*A*). A small subset of tumors showed comparable levels of E-cadherin in tumors and normal tissues (Figure 6*A*, *right set*). In the majority of tumors with elevated E-cadherin levels, there was concomitant elevated β-catenin as well. Thus, overall, most nonmetastatic pancreatic tumors continued to show membranous E-cadherin localization. Next, the β-catenin–E-cadherin complex was examined in the tumors. Previously, the tyrosine phosphorylation of β-catenin has been shown to not only negatively regulate cell–cell adhesion by affecting the β-catenin–E-cadherin complex, but also to contribute to cytoplasmic and nuclear β-catenin (activation) [24,26,27]. No tyrosine phosphorylation on β-catenin was detected in tumors (Figure 6*B*). In addition, the continued association of β-catenin and E-cadherin was evident in all tumors, as seen in a representative blot (Figure 6*B*). The association was proportional to the amount of β-catenin pulled down in the immunoprecipitate. Stoichiometric analysis

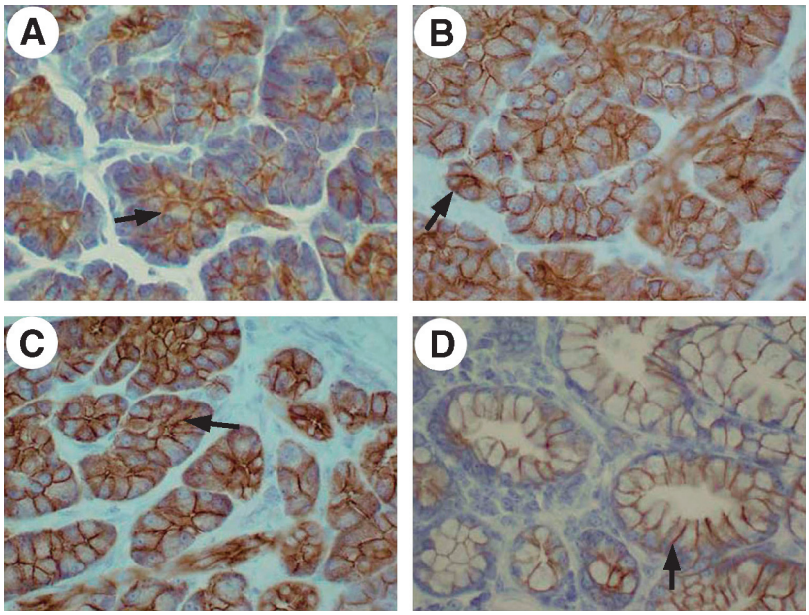

Figure 5. *Continued and increased E-cadherin localization at the membrane in pancreatic tumors. (A) A representative section from normal pancreata shows membranous localization (arrow) of β-catenin with some subcellular stainings. (B and C) Representative analysis from two tumors reveals continued membranous localization (arrow) of E-cadherin with increased intensity and some cytoplasmic staining as well. (D) A representative section from a tumor shows comparable E-cadherin localization or intensity at the membrane (arrow) to the control.*

reveals a 15% to 20% association between these proteins. Although most tumors in this study were nonmetastatic, we observed a continued association of E-cadherin and β-catenin in FT5, which was the only metastatic tumor in our study. Thus, although no changes in β-catenin–E-cadherin association were observed in pancreatic adenocarcinoma, both proteins independently demonstrated an increase in the tumors compared to adjacent or normal pancreata.

Discussion

Aberrations in the Wnt/β-catenin signaling pathway are frequently observed in cancers [28–30]. This pathway is also crucial in the development of normal tissues, such as the skin, brain, mammary gland, liver, and others, and regulates key cellular processes, such as proliferation, apoptosis, and differentiation [10,31]. More recently, its role has been established in pancreatic development as well. Its role in the development of pancreatic adenocarcinoma is controversial due to the lack of a comprehensive analysis of its components in such tumors. One study of a large number of pancreatic adenocarcinomas failed to detect any mutations in the *CTNNB1* gene or nuclear accumulations of β-catenin [16]. Other reports of immunohistochemical analysis of these tumors show a subset with β-catenin accumulation [17,32]. Although the differences observed could be attributed to geographic or idiopathic factors, our present study is a comprehensive analysis of the Wnt/β-catenin pathway in pancreatic tumors in patients.

Activation of the Wnt/β-catenin pathway may proceed via several mechanisms. One such mechanism that brings about β-catenin stabilization is the presence of mutations in the genes encoding for β-catenin, axin, or APC, which interfere with β-catenin phosphorylation and ubiquitination [3,4,8,9]. However, other reports have also demonstrated mutation-independent accumulation and activation of β-catenin [6]. Such mechanisms, although not fully elucidated, involve upstream effectors of β-catenin, such as the Wnt and frizzled, or changes in Wnt pathway modulators, such as frizzled-related proteins, Wnt-inhibitory factor-1, and Dikkopf [33]. Our main goal was to examine any changes in the central component of the canonical Wnt pathway and then to begin to address changes in its upstream effectors, especially in some of the known canonical Wnt and frizzled proteins in the pancreas. The expression of *Wnt* and *frizzled* genes in the pancreas has been explored [20,21,34]. Wnt-1, a classic canonical Wnt, is expressed at low levels in normal pancreata; thus, its alterations could be readily appreciated. In addition, although frizzled-1 and frizzled-2 had been reported in the pancreas as well-known components of the canonical Wnt pathway, we still wanted to address any changes in these proteins in cancer. It was beyond the scope of the present study to examine additional *Wnt* and *frizzled* genes and their products. Yet, another mechanism involved protein–protein interactions at the cell membrane, which was mediated by the tyrosine phosphorylation of β-catenin [26,27,35,36].

This study aims to reconfirm some of the earlier immunohistochemical observations concluding the state of the Wnt/β-catenin pathway in pancreatic adenocarcinoma. Overall, around 65% of all pancreatic tumors showed activation of the canonical Wnt/β-catenin pathway, whereas 11 of 16 paraffin samples of pancreatic tumors showed increased β-catenin accumulation in the cytoplasm and nucleus by immunohistochemistry. An additional 10 of 15 frozen tumors showed an increase in total and nuclear β-catenin proteins. Interestingly, the levels of *c-myc* and *cyclin D1*, known targets of this pathway, did not correlate with elevated β-catenin in all cases. This could be due to β-catenin–independent regulation of these targets, as has been observed in other instances [37–40]. Additionally, an increased tissue/stage specificity of Wnt targets is being identified, suggesting that *c-myc* and *cyclin D1* might not be pancreas-specific targets of this pathway as in the liver [41–43]. Although 2 of 10 frozen tumors showed mutations in exon 3 of *CTNNB1*, the remaining eight tumors demonstrated elevated levels of Wnt-1 and frizzled-2 proteins. This led to decreased phosphorylation of β-catenin at Ser45/Thr41 residues in these tumors and to concurring accumulation and activation of β-catenin. In addition, barring one exception where the axin protein was elevated (perhaps in a compensatory manner) in a tumor, we observed no changes in axin or APC proteins in the tumors or normal pancreata. This failure in the increase of total axin or APC proteins in response to elevated β-catenin levels may further potentiate β-catenin levels in some patients. In addition, this is relevant because we did not identify a decrease in total axin, APC, or GSK3β proteins in the tumors, which would have addressed the mechanism of β-catenin stabilization in the first place. An increase in GSK3β appears to be compensatory because the phosphorylation of β-catenin at Ser45/Thr41 showed a decrease, rather than an expected increase. Again, although the exact mechanism is unclear at this time, increased total GSK3β protein might not reflect a proportional increase in its kinase activity, which might not have changed, especially in the light of the upstream elevated Wnt-1 and frizzled proteins. An alternative explanation can be that, because GSK3β is also a key player in several other pathways such as the insulin, Akt, CREB, and other pathways, the changes observed in its levels in pancreatic adenocarcinoma (total increase) could be secondary to the involvement of any of these pathways [44,45].

β-Catenin–E-cadherin interactions are important in maintaining cell–cell adhesion and in contributing toward β-catenin activation [46]. We observed a consistent increase in both of these proteins in pancreatic tumors. They continued to associate with each other at the membrane, and no tyrosine phosphorylation of β-catenin was detected in the tumors, which was also true in only one metastatic tumor. In addition, the coexisting increase of both proteins in the cytoplasm might also be due to dissociation of these proteins as a complex, as has been reported previously [47]. Although we cannot rule out selection bias, several locally invasive and moderately to poorly differentiated tumors continued to show intact β-catenin–E-cadherin association. Thus, although our study will not be able to rule out the role of the β-catenin–E-cadherin complex in pancreatic tumor invasion

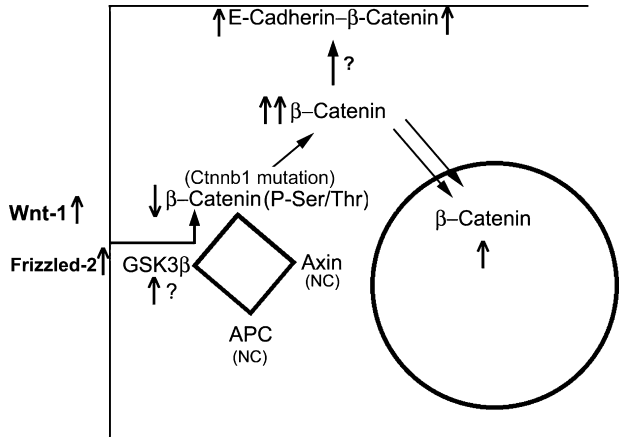

Figure 7. *Summary of changes in the Wnt/β-catenin pathway in pancreatic adenocarcinoma. β-Catenin activation in the form of cytoplasmic stabilization and nuclear translocation occurs secondary to increased Wnt-1 or frizzled-2 proteins or mutations in β-catenin gene (CTNNB1). This is complemented by failure of increases in β-catenin's degradation complex proteins, such as axin and APC. GSK3β increase appears inadequate as reflected by decreased phosphorylation of β-catenin at Ser45 and Thr41. The E-cadherin–β-catenin complex's contribution to cytoplasmic or nuclear β-catenin appears highly unlikely due to continued association and absent tyrosine phosphorylation. A more protective response of this complex to sequester some of the stabilized cytoplasmic β-catenins, especially in nonmetastatic tumors, could be an alternative explanation.*

or metastasis, we conclude its insignificant role in contributing to the free and active β-catenin pool in these tumors.

Thus, all findings of the present study are summarized in Figure 7 and can be highlighted as follows: 1) an increase in Wnt-1 and frizzled-2 proteins results in a decrease in β-catenin serine/threonine phosphorylation and its subsequent accumulation and nuclear translocation; 2) the failure of increase in β-catenin's degradation complex proteins, such as axin and APC, further promotes β-catenin stabilization; and 3) there is only minor, if any, contribution of the E-cadherin–β-catenin complex toward the cytoplasmic pool of β-catenin in these tumors.

Presently, significant efforts are being directed at synthesizing or identifying inhibitors of key pathways that are dysregulated in cancers. Research is aimed at using such inhibitors of several cancer treatments [48–50]. Thus, it is imperative to identify aberrant signaling pathways in specific cancers, which can be targeted for therapy. The Wnt/β-catenin pathway has been discussed previously as a potential therapeutic target [51]. Because we demonstrate aberrant Wnt/β-catenin activation in around 65% of pancreatic adenocarcinomas, there might be a therapeutic role of β-catenin inhibition in these tumors. Several studies in other organs, especially the liver, have correlated β-catenin activation to cell proliferation [22,43]. Although no specific inhibitors of the Wnt/β-catenin pathway are available, we and others have shown the impact of β-catenin inhibition on cell proliferation in the development of tumors by antisense or therapeutic agents [52–54]. Interestingly, Gleevec (STI-571; Novartis, East Hanover, NJ) has been shown to have an anti–β-catenin effect [55]. Unfortunately, such therapy has not shown any benefit in pancreatic adenocarcinoma [56]. The results of our present study clearly demonstrate the reason why it was ineffective in this tumor. As reported by Zhou et al. [55], Gleevec inhibits tyrosine phosphorylation–dependent β-catenin activation, which was never observed in any of the pancreatic tumors analyzed in our study. Thus, this could be at least one of the mechanisms that contributed to the failure of this tyrosine kinase inhibitor to prevent pancreatic tumor progression in patients. Putting it in perspective, our results establish the therapeutic advantage of the identification and use of specific agents in human pancreatic adenocarcinoma that would promote β-catenin degradation and decrease its nuclear translocation in a tyrosine phosphorylation–independent manner. Unpublished reports in our laboratory have identified agents such as celecoxib (Celebrex; Pfizer, New York, NY) and SDX-101 (Salmedix, Inc., San Diego, CA), which induce such a change and may be beneficial in tumors that demonstrate elevated β-catenin levels. This could be one of the factors that might contribute to the therapeutic efficacy of selective COX-2 inhibitors in preclinical pancreatic tumor studies [57,58].

Acknowledgement

We gratefully thank Syd Finkelstein, the staff pathologist, for his help in the interpretation and analysis of immunohistochemical stains.

References

[1] Jemal A, Murray T, Ward E, Samuels A, Tiwari RC, Ghafour A, Feuer EJ, and Thurn MJ (2005). Cancer statistics, 2005. *CA Cancer J Clin* **55** (1), 10–30.

[2] Beger HG, Rau B, Gansauge F, Poch B, and Link KH (2003). Treatment of pancreatic cancer: challenge of the facts. *World J Surg* **27** (10), 1075–1084.

[3] de La Coste A, Romagnolo B, Billuart P, Renard CA, Buendia MA, Soubrane O, Fabre M, Chelly J, Beldjord C, Kahn A, et al. (1998). Somatic mutations of the *beta-catenin* gene are frequent in mouse and human hepatocellular carcinomas. *Proc Natl Acad Sci USA* **95** (15), 8847–8851.

[4] Hugh TJ, Dillon SA, O'Dowd G, Getty B, Pignatelli M, Poston GJ, and Kinsella AR (1999). Beta-catenin expression in primary and metastatic colorectal carcinoma. *Int J Cancer* **82** (4), 504–511.

[5] Jaiswal AS, Kennedy CH, and Narayan S (1999). A correlation of APC and c-myc mRNA levels in lung cancer cell lines. *Oncol Rep* **6** (6), 1253–1256.

[6] Rimm DL, Caca K, Hu G, Harrison FB, and Fearon ER (1999). Frequent nuclear/cytoplasmic localization of beta-catenin without exon 3 mutations in malignant melanoma. *Am J Pathol* **154** (2), 325–329.

[7] Smalley MJ and Dale TC (2001). Wnt signaling and mammary tumorigenesis. *J Mammary Gland Biol Neoplasia* **6** (1), 37–52.

[8] He TC, Sparks AB, Rago C, Hermeking H, Zawel L, da Costa LT, Morin PJ, Vogelstein B, and Kinzler KW (1998). Identification of c-MYC as a target of the APC pathway. *Science* **281** (5382), 1509–1512.

[9] Morin PJ (1999). Beta-catenin signaling and cancer. *Bioessays* **21** (12), 1021–1030.

[10] Cadigan KM and Nusse R (1997). Wnt signaling: a common theme in animal development. *Genes Dev* **11** (24), 3286–3305.

[11] Haegel H, Larue L, Ohsugi M, Fedorov L, Herrenknecht K, and Kemler R (1995). Lack of beta-catenin affects mouse development at gastrulation. *Development* **121** (11), 3529–3537.

[12] Deutsch G, Jung J, Zheng M, Lora J, and Zaret KS (2001). A bipotential precursor population for pancreas and liver within the embryonic endoderm. *Development* **128** (6), 871–881.

[13] Ozturk M (1999). Genetic aspects of hepatocellular carcinogenesis. *Semin Liver Dis* **19** (3), 235–242.

[14] Abraham SC, Wu TT, Klimstra DS, Finn LS, Lee JH, Yeo CJ, Cameron JL, and Hruban RH (2001). Distinctive molecular genetic alterations in sporadic and familial adenomatous polyposis-associated pancreato-

blastomas: frequent alterations in the APC/beta-catenin pathway and chromosome 11p. *Am J Pathol* **159** (5), 1619–1627.
[15] Tanaka Y, Kato K, Notohara K, Nakatani Y, Miyake T, Ijiri R, Nishimata S, Ishida Y, Kigasawa H, Ohama Y, Tsukayama C, Kobayashi Y, and Horie H (2003). Significance of aberrant (cytoplasmic/nuclear) expression of beta-catenin in pancreatoblastoma. *J Pathol* **199** (2), 185–190.
[16] Gerdes B, Ramaswamy A, Simon B, Pietsch T, Bastian D, Kersting M, Moll R, and Bartsch D (1999). Analysis of *beta-catenin* gene mutations in pancreatic tumors. *Digestion* **60** (6), 544–548.
[17] Karayiannakis AJ, Syrigos KN, Polychronidis A, and Simopoulos C (2001). Expression patterns of alpha-, beta- and gamma-catenin in pancreatic cancer: correlation with E-cadherin expression, pathological features and prognosis. *Anticancer Res* **21** (6A), 4127–4134.
[18] Aberle H, Bauer A, Stappert J, Kispert A, and Kemler R (1997). Beta-catenin is a target for the ubiquitin–proteasome pathway. *EMBO J* **16** (13), 3797–3804.
[19] Barker N, Morin PJ, and Clevers H (2000). The Yin–Yang of TCF/beta-catenin signaling. *Adv Cancer Res* **77,** 1–24.
[20] Heller RS, Dichmann DS, Jensen J, Miller C, Wong G, Madsen OD, and Serup P (2002). Expression patterns of Wnts, frizzleds, sFRPs, and misexpression in transgenic mice suggesting a role for Wnts in pancreas and foregut pattern formation. *Dev Dyn* **225** (3), 260–270.
[21] Heller RS, Klein T, Ling Z, Heimberg H, Katoh M, Madsen OD, and Serup P (2003). Expression of *Wnt*, *frizzled*, *sFRP*, and *DKK* genes in adult human pancreas. *Gene Expr* **11** (3–4), 141–147.
[22] Micsenyi A, Tan X, Sneddon T, Luo JH, Michalopoulos GK, and Monga SP (2004). Beta-catenin is temporally regulated during normal liver development. *Gastroenterology* **126** (4), 1134–1146.
[23] Monga SP, Pediaditakis P, Mule K, Stolz DB, and Michalopoulos GK (2001). Changes in WNT/beta-catenin pathway during regulated growth in rat liver regeneration. *Hepatology* **33** (5), 1098–1109.
[24] Behrens J, Vakaet L, Friis R, Winterhager E, Van Roy F, Mareel MM, and Birchmeier W (1993). Loss of epithelial differentiation and gain of invasiveness correlates with tyrosine phosphorylation of the E-cadherin/beta-catenin complex in cells transformed with a temperature-sensitive *v-SRC* gene. *J Cell Biol* **120** (3), 757–766.
[25] Kemler R (1993). From cadherins to catenins: cytoplasmic protein interactions and regulation of cell adhesion. *Trends Genet* **9** (9), 317–321.
[26] Danilkovitch-Miagkova A, Miagkov A, Skeel A, Nakaigawa N, Zbar B, and Leonard EJ (2001). Oncogenic mutants of RON and MET receptor tyrosine kinases cause activation of the beta-catenin pathway. *Mol Cell Biol* **21** (17), 5857–5868.
[27] Monga SP, Mars WM, Pediaditakis P, Bell A, Mule K, Bowen WC, Wang X, Zarnegar R, and Michalopoulos GK (2002). Hepatocyte growth factor induces Wnt-independent nuclear translocation of beta-catenin after Met-beta-catenin dissociation in hepatocytes. *Cancer Res* **62** (7), 2064–2071.
[28] Giles RH, van Es JH, and Clevers H (2003). Caught up in a Wnt storm: Wnt signaling in cancer. *Biochim Biophys Acta* **1653** (1), 1–24.
[29] Lustig B and Behrens J (2003). The Wnt signaling pathway and its role in tumor development. *J Cancer Res Clin Oncol* **129** (4), 199–221.
[30] Moon RT, Bowerman B, Boutros M, and Perrimon N (2002). The promise and perils of Wnt signaling through beta-catenin. *Science* **296** (5573), 1644–1646.
[31] Peifer M and Polakis P (2000). Wnt signaling in oncogenesis and embryogenesis—a look outside the nucleus. *Science* **287** (5458), 1606–1609.
[32] Lowy AM, Fenoglio-Preiser C, Kim OJ, Kordich J, Gomez A, Knight J, James L, and Groden J (2003). Dysregulation of beta-catenin expression correlates with tumor differentiation in pancreatic duct adenocarcinoma. *Ann Surg Oncol* **10** (3), 284–290.
[33] Hsieh JC, Kodjabachian L, Rebbert ML, Rattner A, Smallwood PM, Samos CH, Nusse R, Dawid IB, and Nathans J (1999). A new secreted protein that binds to Wnt proteins and inhibits their activities. *Nature* **398** (6726), 431–436.
[34] Murtaugh LC, Law AC, Dor Y, and Melton DA (2005). Beta-catenin is essential for pancreatic acinar but not islet development. *Development* **132** (21), 4663–4674.
[35] Papkoff J and Aikawa M (1998). WNT-1 and HGF regulate GSK3 beta activity and beta-catenin signaling in mammary epithelial cells. *Biochem Biophys Res Commun* **247** (3), 851–858.
[36] Rosario M and Birchmeier W (2003). How to make tubes: signaling by the Met receptor tyrosine kinase. *Trends Cell Biol* **13** (6), 328–335.
[37] Abdollahi A, Gruver BN, Patriotis C, and Hamilton TC (2003). Identification of epidermal growth factor–responsive genes in normal rat ovarian surface epithelial cells. *Biochem Biophys Res Commun* **307** (1), 188–197.
[38] Ko TC, Sheng HM, Reisman D, Thompson EA, and Beauchamp RD (1995). Transforming growth factor-beta 1 inhibits cyclin D1 expression in intestinal epithelial cells. *Oncogene* **10** (1), 177–184.
[39] Schwabe RF, Bradham CA, Uehara T, Hatano E, Bennett BL, Schoonhoven R, and Brenner DA (2003). c-Jun-N-terminal kinase drives cyclin D1 expression and proliferation during liver regeneration. *Hepatology* **37** (4), 824–832.
[40] Tarbe N, Losch S, Burtscher H, Jarsch M, and Weidle UH (2002). Identification of rat pancreatic carcinoma genes associated with lymphogenous metastasis. *Anticancer Res* **22** (4), 2015–2027.
[41] Cadoret A, Ovejero C, Saadi-Kheddouci S, Souil E, Fabre M, Romagnolo B, Kahn A, and Perret C (2001). Hepatomegaly in transgenic mice expressing an oncogenic form of beta-catenin. *Cancer Res* **61** (8), 3245–3249.
[42] Cadoret A, Ovejero C, Terris B, Souil E, Levy L, Lamers WH, Kitajewski J, Kahn A, and Perret C (2002). New targets of beta-catenin signaling in the liver are involved in the glutamine metabolism. *Oncogene* **21** (54), 8293–8301.
[43] Tan X, Apte U, Micsenyi A, Kotsagrelos E, Luo JH, Ranganathan S, Monga DK, Bell A, Michalopoulos GK, and Monga SP (2005). Epidermal growth factor receptor: a novel target of the Wnt/beta-catenin pathway in liver. *Gastroenterology* **129** (1), 285–302.
[44] Grimes CA and Jope RS (2001). CREB DNA binding activity is inhibited by glycogen synthase kinase-3 beta and facilitated by lithium. *J Neurochem* **78** (6), 1219–1232.
[45] Noda S, Kishi K, Yuasa T, Hayashi H, Ohnishi T, Miyata I, Nishitani H, and Ebina Y (2000). Overexpression of wild-type Akt1 promoted insulin-stimulated p70S6 kinase (p70S6K) activity and affected GSK3 beta regulation, but did not promote insulin-stimulated GLUT4 translocation or glucose transport in L6 myotubes. *J Med Invest* **47** (1–2), 47–55.
[46] Lilien J and Balsamo J (2005). The regulation of cadherin-mediated adhesion by tyrosine phosphorylation/dephosphorylation of beta-catenin. *Curr Opin Cell Biol* **17** (5), 459–465.
[47] Kamei T, Matozaki T, Sakisaka T, Kodama A, Yokoyama S, Peng YF, Nakano K, Takaishi K, and Takai Y (1999). Coendocytosis of cadherin and c-Met coupled to disruption of cell–cell adhesion in MDCK cells—regulation by Rho, Rac and Rab small G proteins. *Oncogene* **18** (48), 6776–6784.
[48] Bergers G, Song S, Meyer-Morse N, Bergsland E, and Hanahan D (2003). Benefits of targeting both pericytes and endothelial cells in the tumor vasculature with kinase inhibitors. *J Clin Invest* **111** (9), 1287–1295.
[49] Ritter CA and Arteaga CL (2003). The epidermal growth factor receptor-tyrosine kinase: a promising therapeutic target in solid tumors. *Semin Oncol* **30** (1), 3–11 (Suppl 1).
[50] Sausville EA, Elsayed Y, Monga M, and Kim G (2003). Signal transduction–directed cancer treatments. *Annu Rev Pharmacol Toxicol* **43,** 199–231.
[51] Li H, Pamukcu R, and Thompson WJ (2002). Beta-catenin signaling: therapeutic strategies in oncology. *Cancer Biol Ther* **1** (6), 621–625.
[52] Monga SP, Monga HK, Tan X, Mule K, Pediaditakis P, and Michalopoulos GK (2003). Beta-catenin antisense studies in embryonic liver cultures: role in proliferation, apoptosis, and lineage specification. *Gastroenterology* **124** (1), 202–216.
[53] Sodhi D, Micsenyi A, Bowen WC, Monga DK, Talavera JC, and Monga SP (2005). Morpholino oligonucleotide–triggered beta-catenin knockdown compromises normal liver regeneration. *J Hepatol* **43** (1), 132–141.
[54] Yao M, Kargman S, and Lam EC, Kelly CR, Zheng Y, Luk P, Kwong E, Evans JF, Wolfe MM (2003). Inhibition of cyclooxygenase-2 by rofecoxib attenuates the growth and metastatic potential of colorectal carcinoma in mice. *Cancer Res* **63** (3), 586–592.
[55] Zhou L, An N, Haydon RC, Zhou QX, Cheng HW, Peng Y, Jiang W, Luu HH, Vanichakarn P, Szatkowski JP, et al. (2003). Tyrosine kinase inhibitor STI-571/Gleevec down-regulates the beta-catenin signaling activity. *Cancer Lett* **193** (2), 161–170.
[56] Chen J, Rocken C, Nitsche B, Hosius C, Gschaidmeier H, Kahl S, Malfertheiner P, Ebert MP (2005). The tyrosine kinase inhibitor imatinib fails to inhibit pancreatic cancer progression. *Cancer Lett.*
[57] Schuller HM, Zhang L, Weddle DL, Castonguay A, Walker K, and Miller MS (2002). The cyclooxygenase inhibitor ibuprofen and the FLAP inhibitor MK886 inhibit pancreatic carcinogenesis induced in hamsters by transplacental exposure to ethanol and the tobacco carcinogen NNK. *J Cancer Res Clin Oncol* **128** (10), 525–532.
[58] Tseng WW, Deganutti A, Chen MN, Saxton RE, and Liu CD (2002). Selective cyclooxygenase-2 inhibitor rofecoxib (Vioxx) induces expression of cell cycle arrest genes and slows tumor growth in human pancreatic cancer. *J Gastrointest Surg* **6** (6), 838–843 (discussion 44).